MANY-BODY THEORY OF THE ELECTROWEAK NUCLEAR RESPONSE*

Omar Benhar

INFN and Department of Physics, Università "La Sapienza"
I-00185 Roma, Italy

(Received June 23, 2006)

I discuss the theoretical treatment of the electroweak nuclear response based on nonrelativistic nuclear many-body theory. This approach allows for a unified parameter-free description of a variety of kinematical regions relevant to many neutrino experiments. Selected applications to electron- and neutrino–nucleus scattering in the impulse approximation regime are analyzed.

PACS numbers: 24.10.Cn, 25.30.Fj, 61.12.Bt

1. Introduction

In view of the rapid development of neutrino physics, leading to significant improvements in the experimental accuracy, the treatment of nuclear effects in data analysis is now regarded as one of the main sources of systematic uncertainty [1, 2].

Theoretical descriptions of the nuclear response to electroweak probes necessarily imply two different sources of uncertainty. First, due to the complexity of the fundamental theory of strong interactions, one has to rely on dynamical models, based on nucleon and meson degrees of freedom and effective interactions. Second, the calculation of transition matrix elements between nuclear states necessarily involves approximations for targets having nuclear mass number $A > 4$.

In Nuclear Many-Body Theory (NMBT) the nucleus is viewed as a collection of pointlike protons and neutrons, whose dynamics are described by the nonrelativistic Hamiltonian

$$H = \sum_i \frac{\boldsymbol{p}_i^2}{2m} + \sum_{j>i} v_{ij} + \sum_{k>j>i} V_{ijk} \ , \tag{1.1}$$

* Presented at the XX Max Born Symposium "Nuclear Effects in Neutrino Interactions", Wrocław, Poland, December 7–10, 2005.

where $\boldsymbol{p}_i$ and m denote the momentum of the i-th nucleon and the nucleon mass, respectively. The two body potential v_{ij} is determined by fitting deuteron properties and ~ 4000 precisely measured nucleon–nucleon (NN) scattering phase shitfs [3], while inclusion of the three-nucleon interaction $V_{ijk} \ll v_{ij}$ is required to account for the binding energy of the three-nucleon systems [4].

The many body Schrödinger equation associated with the Hamiltonian of Eq. (1.1) can be solved exactly, using stochastic methods, for nuclei with mass number up to 10. The resulting energies of the ground and low-lying excited states are in excellent agreement with experimental data [5].

It is very important to realize that in NMBT the dynamics is fully determined by the properties of exactly solvable system, and does not suffer from the uncertainties involved in many-body calculations. Once the nuclear Hamiltonian is fixed, calculations of nuclear observables for a variety of systems, ranging from deuteron to neutron stars, can be carried out without making use of any adjustable parameters.

The theoretical description of the electroweak nuclear response based on NMBT is outlined in Section 2, whereas Section 3 focuses on the region of high momentum transfer, where the impulse approximation (IA) scheme becomes applicable. Sections 4 and 5 are devoted to the analysis of selected applications to electron– and neutrino–nucleus scattering processes, respectively, while conclusions and prospects are stated in Section 6.

2. The nuclear electroweak response

The scattering cross section of the process

$$\ell + A \to \ell' + X \,, \tag{2.1}$$

where ℓ and ℓ' denote either a charged lepton or a neutrino and X represents the undetected hadronic final state, can be written in the form

$$d\sigma_A \propto L_{\mu\nu} W_A^{\mu\nu} \,. \tag{2.2}$$

In the above equation, the tensor $L_{\mu\nu}$ is determined by the lepton kinematics, whereas all the information on nuclear dynamics is contained in the response tensor

$$W_A^{\mu\nu}(q) = \sum_n \langle 0|J_A^{\mu\,\dagger}(q)|n\rangle\langle n|J_A^{\nu}(q)|0\rangle \delta^{(4)}(p_0 + q - p_n) \,, \tag{2.3}$$

whose calculation requires the knowledge of the target ground and excited states, $|0\rangle$ and $|n\rangle$, as well as of the nuclear electroweak current J_A^μ.

At moderate momentum transfer ($|\boldsymbol{q}| < 500$ MeV) exact calculations of $W_A^{\mu\nu}$ can be carried out for $A \leq 4$ using integral transform techniques [6,7]. Accurate results can also be obtained in the $A \to \infty$ limit using Correlated Basis Function (CBF) perturbation theory [8,9].

The CFB approach is based on the use of the complete set of *correlated* states

$$|n\rangle = F|n_{\rm MF}\rangle\,, \tag{2.4}$$

where $|n_{\rm MF}\rangle$ is a state obtained from the mean-field approximation, *e.g.* a nuclear shell-model wave function, while the operator F, which takes into account NN correlations induced by the strong nuclear forces, is generally written in the form

$$F = \mathcal{S} \prod_{j>i} f_{ij}\,. \tag{2.5}$$

The structure of the two-nucleon correlation operator f_{ij} reflects the complexity of the NN potential, which is known to be non spherically symmetric and strongly spin–isospin dependent. The symmetrization operator $\mathcal{S}$ is needed to preserve the symmetry of the state $|n\rangle$, as in general $[f_{ij}, f_{jk}] \neq 0$.

The Hamiltonian of Eq. (1.1) can be split according to

$$H = H_0 + H_I\,, \tag{2.6}$$

where H_0 and H_I denote its diagonal and non diagonal part in the correlated basis, respectively, *i.e.*

$$\langle m|H_0|n\rangle = \delta_{mn}\langle m|H|n\rangle\,, \tag{2.7}$$

$$\langle m|H_I|n\rangle = (1-\delta_{mn})\langle m|H|n\rangle\,. \tag{2.8}$$

If the correlated states have large overlaps with the eigenstates of H, the matrix elements (2.8) are small and the perturbative expansion in powers of H_I is rapidly convergent.

CBF perturbation theory has been used to calculate the electromagnetic response of infinite nuclear matter for momentum transfers up to ~ 500 MeV [9]. The results, obtained including the contributions of one particle-one hole and two particle–two hole intermediate states in Eq. (2.3), clearly show that the effects of short range NN correlations are large.

Long range correlations are also known to be important at low momentum transfer ($|\boldsymbol{q}| < 200$ MeV), but their description within CBF involves severe difficulties. However, implementation of effective interactions extracted from the CBF results in the standard Random Phase Approximation scheme [10] may provide a computationally viable approach allowing for a consistent treatment of short and long range correlations.

3. The impulse approximation regime

At large momentum transfer the nonrelativistic approximation breaks down. However, when the space resolution of the beam particle, $\sim 1/|\boldsymbol{q}|$, becomes much smaller than the average distance between nucleons in the target, the IA regime sets in. Under these conditions, the nuclear cross section reduces to the incoherent sum of elementary scattering processes involving individual *bound* nucleons. Neglecting final state interactions (FSI) between the struck particle and the spectator nucleons one can then rewrite Eq. (2.3) in the simple form

$$W_A^{\mu\nu}(q) = \sum_i \int d^4k \ \left(\frac{m}{E_{\boldsymbol{k}}}\right) P_i(k) \widetilde{w}_i^{\mu\nu}(k,q)\,, \tag{3.1}$$

where the spectral function $P_i(k)$ yields the energy and momentum distribution of the i-th nucleon, whose electroweak structure is described by the tensor $\widetilde{w}_i^{\mu\nu}$.

Accurate calculations of the spectral function have been carried out for light nuclei [11–13] and infinite nuclear matter [14, 15]. The proton spectral functions of medium-heavy nuclei have also been modeled using the Local Density Approximation (LDA) [16, 17], in which the experimental information obtained from electron-induced nucleon knock out measurements is combined with the results of theoretical calculations of the nuclear matter spectral function carried out at different densities.

The tensor $\widetilde{w}_i^{\mu\nu}$ can be expressed in terms of the proton and neutron structure functions obtained from lepton–proton and lepton–deuteron data, the effects of nuclear binding being accounted for through a shift of the energy transfer [18].

The effect of FSI, neglected in Eq. (3.1), has long been recognized to be sizable. In inclusive processes it amounts to *(i)* an energy shift of the cross section, due to the fact that the struck nucleon moves in the average potential generated by the spectator particles and *(ii)* a redistribution of the strength, leading to the quenching of the quasi-elastic peak and the enhancement of the tails, to be ascribed to the occurrence of NN scattering processes coupling the one particle-one hole final state to more complex n particle–n hole configurations.

A theoretical approach to describe FSI, based on NMBT and a generalization of Glauber theory of high energy proton scattering [19], has been proposed in the early 90s [20]. This treatment of FSI, generally referred to as Correlated Glauber Approximation (CGA) rests on the premises that *(i)* the struck nucleon moves along a straight trajectory with constant velocity (eikonal approximation), and *(ii)* the spectator nucleons are seen by the struck particle as a collection of fixed scattering centers (frozen approximation).

4. Electron–nucleus scattering

The approach outlined in Section 3 has been widely and successfully applied to the analysis of electron–nucleus scattering data (for a recent review see, *e.g.*, Ref. [21]).

In Ref. [22], it has been employed to calculate the inclusive electron scattering cross sections off oxygen at beam energies ranging between 700 and 1200 MeV and electron scattering angle 32°. In this kinematical region, relevant to many neutrino experiments, single nucleon knock out is the dominant reaction mechanism and both quasi-elastic and inelastic processes, leading to the appearance of hadrons other than protons and neutrons, must be taken into account.

Comparison between theoretical results and the experimental data of Ref. [23] shows that, while the data in the region of the quasi-elastic peak are accounted for with an accuracy better than ~ 10 %, theory fails to explain the measured cross sections at larger electron energy loss, where Δ production dominates.

As an example, Fig. 1 shows the results of Ref. [22] at beam energy 700 and 1200 MeV. For reference, the results of the Fermi gas (FG) model corresponding to Fermi momentum $p_{\rm F} = 225$ MeV and average removal energy $\epsilon = 25$ MeV are also shown. Theoretical calculations have been carried out using the Höhler–Brash parameterization of the nucleon form factors [24,25] in the quasi-elastic channel and the Bodek and Ritchie parametrization of the proton and neutron structure functions in the inelastic channels [26].

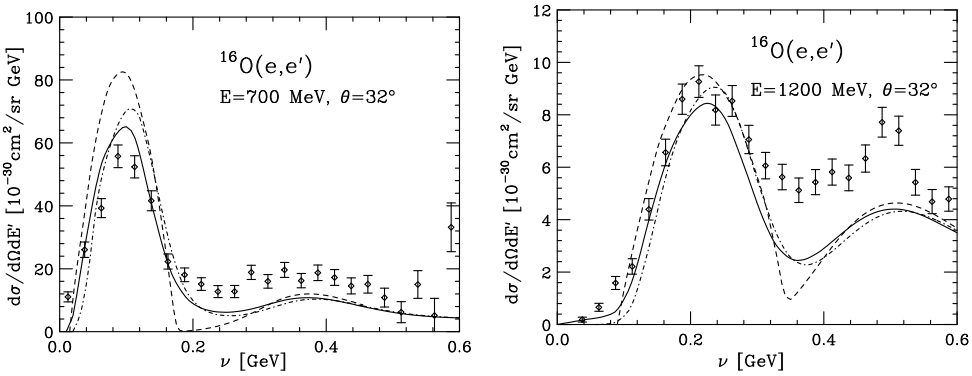

Fig. 1. Cross section of the process $^{16}{\rm O}(e,e')$ at scattering angle 32° and beam energy 700 MeV (left panel) and 1200 MeV (right panel). Solid lines: full calculation, carried out within the approach described in Section 3. Dot-dashed lines: IA calculation, carried out neglecting FSI effects. Dashed lines: FG model with $p_{\rm F} = 225$ MeV and $\epsilon = 25$ MeV. The data are taken from Ref. [23].

The authors of Ref. [22] argued that the disagreement between theory and data in the Δ production region is likely to be imputable to deficiencies in the description of the nucleon structure functions at low Q^2. This conclusion is supported by the analysis recently carried out in Ref. [27].

The results of Fig. 1 clearly illustrate the inadequacy of the FG model, often employed in the analysis of neutrino experiment, to describe the data. Fixing the model parameters to reproduce the quasi-elastic peak at 1200 MeV leads to a 40% discrepancy at 700 MeV. On the other hand, the approach based in NMBT, involving no adjustable parametes, provides a satisfactory description of the quasi-elastic region for both kinematics.

5. Charged current neutrino–nucleus scattering

The approach based on NMBT can be readily generalized to describe charged current neutrino–nucleus interactions [22]. It has to be pointed out, however, that, while including dynamical correlations in the final state, it does not take into account statistical correlations, leading to Pauli blocking of the phase space available to the knocked out nucleon.

The effect of Pauli blocking, which can be included through a modification of the spectral function [22], is hardly visible in the differential electron–nucleus cross section discussed in Section 4, corresponding to $Q^2 > 0.2$ GeV^2 at the quasi-elastic peak. On the other hand, it appears to be very large at lower values of Q^2.

Figure 2 shows the calculated differential cross section $d\sigma/dQ^2$ for scattering of 1 GeV electron neutrinos off oxygen. The dashed and dot-dashed

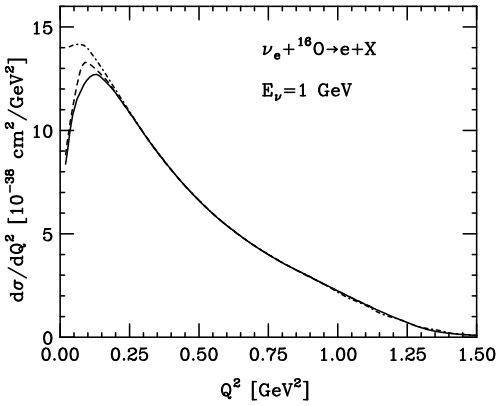

Fig. 2. Differential cross section $d\sigma/dQ^2$ for scattering of 1 GeV electron neutrinos off oxygen. The dot-dashed line shows the IA results, while the solid and dashed lines have been obtained taking into account Pauli blocking with and without inclusion of dynamical FSI, respectively.

lines correspond to the IA results with and without inclusion of Pauli blocking, respectively. The effect of Fermi statistic in suppressing scattering shows up at $Q^2 \sim 0.2$ GeV^2 and becomes dominant at lower Q^2. The results of the full calculation, in which dynamical FSI are also included, are displayed as a full line. The results of Fig. 2 suggest that Pauli blocking and FSI may explain the deficit of the measured cross section at low Q^2 with respect to the predictions of Monte Carlo simulations [28].

6. Conclusions and prospects

The approach based on NMBT provides a unified parameter-free description of the electroweak nuclear response in a variety of kinematical regions relevant to many neutrino experiments.

Thanks to the availability of reliable spectral functions, accurate calculations of the cross sections in the IA regime can now be carried out including the effects of short range NN correlations. Correlation effects can also be consistenly included in the treatment of FSI between the struck nucleon and the spectator particles.

Comparison to electron–nucleus scattering data shows that, while the region of the quasi-elastic peak is described with an accuracy of ~ 10 %, theory still fails to account for the measured cross sections at larger energy transfer. Better models of the nucleon structure functions at $Q^2 < 0.5$ GeV^2 appear to be needed for a fully quantitative understanding of the Δ production region. The role of meson exchange currents, which are known to provide a significant amount of strength in the dip region between the quasi-elastic and the Δ production peak, also needs to be carefully investigated.

As a final remark, it has to be pointed out that the possibility of using the approach based on NMBT in the analysis of neutrino experiments largely depends on the ability to implement its elements in Monte Carlo simulations.

Assuming, for the sake of simplicity, that the elementary weak interaction vertex in the nuclear medium be the same as in free space, a realistic simulation of neutrino–nucleus scattering requires the energy and momentum probability distribution of the nucleons, needed to specify the initial state, as well as their distribution in space and the medium modified hadronic cross section, needed for the description of FSI.

Studies based on NMBT and stochastic methods to solve the many-body Schrödinger equation appear to be capable of providing access to all the above quantities for a variety of nuclear targets.

REFERENCES

[1] Proceedings of NuInt01, eds. J.G. Morfin, and M. Sakuda, Y. Suzuki, *Nucl. Phys. B (Proc. Suppl.)* **112** (2002).

[2] Proceedings of NuInt04, eds. F. Cavanna, P. Lipari, C. Keppel and M. Sakuda, *Nucl. Phys. B (Proc. Suppl.)* **139** (2005).

[3] R.B. Wiringa, V.G.J. Stoks, R. Schiavilla, *Phys. Rev.* **C51**, 38 (1995).

[4] P.S. Pudliner, V.R. Pandharipande, J. Carlson, S.C. Pieper, R.B. Wiringa, *Phys. Rev.* **C56**, 1720 (1997).

[5] S.C. Pieper, R.B. Wiringa, *Annu. Rev. Nucl. Part. Sci.* **51**, 53 (2001).

[6] J. Carlson, R. Schiavilla, *Phys. Rev. Lett.* **68**, 3682 (1992).

[7] V.D. Efros, W. Leidemann, G. Orlandini, *Phys. Lett.* **B338**, 130 (1994).

[8] S. Fantoni, V.R. Pandharipande, *Nucl. Phys.* **A473**, 234 (1987).

[9] A. Fabrocini, S. Fantoni, *Nucl. Phys.* **A503**, 375 (1989).

[10] G. Co', *Acta Phys. Pol. B* **37**, 2235 (2006), these proceedings.

[11] A.E.L. Dieperink, T. de Forest, I. Sick, R.A. Brandenburg, *Phys. Lett.* **B63**, 261 (1976).

[12] C. Ciofi degli Atti, E. Pace, G. Salmè, *Phys. Rev.* **C21**, 805 (1980).

[13] H. Meier-Hajduk, C. Hajduk, P.U. Sauer, W. Theis, *Nucl. Phys.* **A395**, 332 (1983).

[14] O. Benhar, A. Fabrocini, F. Fantoni, *Nucl. Phys.* **A505**, 267 (1989).

[15] A. Ramos, A. Polls, W.H. Dickhoff, *Nucl. Phys.* **A503**, 1 (1989).

[16] O. Benhar, A. Fabrocini, S. Fantoni, I. Sick, *Nucl. Phys.* **A579**, 493 (1994).

[17] A.M. Ankowski, J.T. Sobczyk, `nucl-th/0512004`; A.M. Ankowski, *Acta Phys. Pol. B* **37**, 2259 (2006) these proceedings.

[18] T. de Forest, Jr., *Nucl. Phys.* **A392**, 232 (1983).

[19] R.J. Glauber, in *Lectures in Theoretical Physics*, eds. W.E. Brittin *et al.*, Interscience, New York 1959.

[20] O. Benhar, A. Fabrocini, S. Fantoni, G.A. Miller, V.R. Pandharipande, I. Sick, *Phys. Rev.* **C44**, 2328 (1991).

[21] O. Benhar, D. Day, I. Sick, `nucl-ex/0603029`, to be published in *Rev. Mod. Phys.*

[22] O. Benhar, N. Farina, H. Nakamura, M. Sakuda, R. Seki, *Phys. Rev.* **D72**, 053005 (2005).

[23] M. Anghinolfi *et al.*, *Nucl. Phys.* **A602**, 405 (1996).

[24] G. Höhler *et al.*, *Nucl. Phys.* **B114**, 505 (1976).

[25] E.J. Brash, A. Kozlov, Sh. Li, G.M. Huber, *Phys. Rev.* **C65**, 051001(R) (2002).

[26] A. Bodek, J.L. Ritchie, *Phys. Rev.* **D23**, 1070 (1981).

[27] O. Benhar, D. Meloni, `hep-ph/0604071` submitted to *Phys. Rev. Lett.*

[28] T. Ishida, *Nucl. Phys. B Proc. Suppl.*, **112**, 132 (2002).